Effect of flax fibers on early age shrinkage and cracking of earth concrete

Nathalie Kouta, Jacqueline Saliba, Nadia Saiyouri

Effect of flax fibers on early age shrinkage and cracking of earth concrete

KOUTA Nathalie *, SALIBA Jacqueline , SAIYOURI Nadia

Université de Bordeaux, UMR 5295, Institut de Mécanique et d'Ingénierie (I2M), CNRS, Esplanade des Arts et Metiers, 33405 Talence, France

Abstract. Earth concrete or concrete based on soil materials presents a high percentage of fine particles (clay) which makes it susceptible to plastic shrinkage cracking in its fresh state that affects its durability. In this study, natural flax fibers with different mass percentages (0%, 0.3% and 0.6%) and lengths (12 mm, 24 mm, 50 mm) have been added to earth concrete in order to study their effect on plastic shrinkage and cracking at early age. The effect of flax fibers on the mechanical properties of hardened earth concrete has been first investigated. Free horizontal plastic shrinkage has also been measured in parallel with the evaporation rate, the capillary pressure and the temperature of earth concrete at early age. Furthermore, restrained plastic shrinkage tests have been conducted according to ASTM C1579-13 standard. The Digital Image Correlation technique have been used to monitor the strain distribution and crack width during the first 24 hours after casting. The results show a reduction of the total free plastic shrinkage at early age with the addition of flax fibers. In addition, flax fibers reduce the strain localization of restrained shrinkage and the plastic shrinkage cracking.

Keywords: earth concrete; flax fibers; plastic shrinkage; cracking; Digital Image Correlation.

1. Introduction

During the last decades, a large quantity of natural resources has been consumed by the construction sector. In addition, a large quantity of waste and an intensive emission of CO_2 have been generated [1] which have a significant impact on the environment and participate in climate change [2,3]. Thus, the need of using ecological and sustainable materials is becoming an obligation in the construction field in order to reduce its contribution in the global pollution and the danger that can result from it. Earth concrete is an ecological material and can be an alternative to conventional concrete for

structures that do not require high mechanical performances but rather good thermal and acoustic characteristics [4].

Earth construction has been used for thousands of years in different forms such as: wattle and daub, cob, rammed earth, adobe, compressed earth blocks… [4, 5]. Currently, more than two billion people live in earth constructions [6]. The majority of these constructions are located in less developed countries and rural areas due to the low cost of earth-based materials and its availability [7, 8]. Earth constructions are essentially composed of a raw material, the soil which is a non-manufactured, recyclable, inexpensive and local material which allows to reduce the cost and the energy for transportation and production [5]. In addition, the air and temperature regulation properties of earth concrete promote to a healthier and more comfortable indoor environment by moderating the indoor humidity variations in comparison to conventional construction materials [5]. Consequently, the economic benefits and ecological properties of earth materials incite new research in this field in many developed countries (Europe, US, UK…) [8].

The stabilization of soil has been first realized with lime then with cement and other pozzolanic materials (fly ash, silica fume, geopolymer, etc.) or even a mix of several binders together [9, 10, 11, 12]. The lime is essentially used to enhance the maneuverability and the geotechnical properties of the soil [13, 14, 15, 16]. The treatment of clay with lime is primarily responsible of the improvement of soil workability, the increase of the plastic limits and the reduction of the clays volume change [15]. In addition, the lime increases the durability of the soil as it influences the soil permeability [17] and the durability of the soil in contact with water [18]. In addition, it allows to increase the cohesion and the long term strength due to pozzolanic reactions [13, 19]. In fact, many studies have showed the formation of hydrates during the treatment of soil with lime [13, 15, 20, 21]. The same hydrates that are formed during the hydration of cement and more specifically the hydration of calcium silicates (C3S, C2S) and calcium aluminates (C3A, C4AF) are observed: calcium silicate hydrates (CSH), calcium aluminate hydrates (CAH) and calcium alumina silicate hydrate (CASH). Pozzolanic reactions begin to occur between the calcium from the lime and the tetrahedral and octahedral layers of the clay sheets as a result of cation exchange reactions. Consequently, these reactions take place at

55 the edges of clay particles with an excess of cations in the solution. These hydrates increase the
56 cohesive strength between the clay particles and thus the mechanical properties [21, 22].
57 On the other hand, the cement is used to enhance the mechanical properties and the durability of earth
58 concrete due to hydration reactions [22, 24]. In fact, earth concrete is a vulnerable material mainly
59 when it is in contact with water. The use of cement and other binders is a common practice [25] and
60 has been recommended by many researchers. Note here, that the effect of cement on the mechanical
61 properties depends highly on the mineral composition of soil; while the kaolinite increased slightly
62 the compressive strength, the montmorillonite lowered it same as biedellite but with a lower rate [26].
63 In addition, even though in some cases the addition of binders can decrease the mechanical
64 properties, however it decreases the possibility of biological development [27].
65
66 In recent years, researchers have focused on finding easier and more common methods to use
67 stabilized earth materials in the construction field and on the characterization of their mechanical,
68 physical and thermal properties [9, 12, 28, 29]. However, few research studied the behavior of earth
69 concrete at early age [30]. Thus, additional studies are required to better understand the behavior of
70 earth concrete in its fresh state.
71 Earth based materials present a high shrinkage rate due to the presence of fine particles and thus
72 cracking sensibility during drying when concrete is restrained [29, 30]. Early age shrinkage of
73 concrete starts directly right after concrete casting due to plastic settlement, autogenous shrinkage
74 and plastic shrinkage. This shrinkage can lead to an early age cracking that can, in addition to the
75 aesthetical problem, affect the long-term durability of the concrete [31]. During the fresh state of
76 concrete and before its hardening, plastic shrinkage can be explained by different mechanisms and
77 different phases can be distinguished [32]. The phenomena begin when the solid particles begin to
78 settle accompanied with the rise of water to the surface leading to a plastic settlement [33]. Then,
79 when bleeding water evaporates, plastic shrinkage starts [33]. In fact, the drying surfaces generate a
80 hydraulic pressure in the porous network due to the development of water menisci. Capillary pressure
81 leads to both vertical and horizontal deformations in concrete. If tensile stresses caused by restrained
82 shrinkage exceed the maximum stress capacity of concrete, cracks occur [34]. Plastic shrinkage

cracking depends on the environmental conditions where concrete is conserved after casting in addition to structure geometry and material composition [33, 35, 36]. The cracking risk of earth concrete at early age is high because of its relatively low strength and the significant plastic shrinkage rate.

The addition of fibers with arbitrary distribution is a successful technique to control crack initiation and propagation in concrete at its early age due to plastic and autogenous shrinkage [33]. Adding fibers to concrete allows to disperse cracking, to improve the strain capacity of fresh concrete by providing bridging forces across the cracks, to reduce aggregate segregation and to increase the tensile strength of concrete at its early age [37, 38, 39]. Natural fibers have been widely used in earth construction with the aim to enhance the performance of earth concrete. The addition of fibers may increase the strength and the ductility, lighten the earthen construction materials and reduce plastic shrinkage at early age by limiting the crack development due to stress redistribution [9, 29, 40]. These fibers vary in type, chemical properties, shape, size, source, strength, elasticity, water absorption rate … [41] which may affect the plastic shrinkage cracking in addition to the effect of the fibers percentage and the cohesion between fibers and concrete matrix [9, 33]. Several studies have tested the effect of different types of fibers on the physical and mechanical properties of earth-based concrete [28, 42, 43]. Flax fibers are natural ecological fibers with low-cost in comparison to other types of fibers as steel fibers and synthetic fibers. They are generally produced as waste materials during the agriculture process with a low transformation process. Thus, flax fibers have been used in this study due to their ecological properties and their good compatibility with earth concrete properties.

The aim of this paper is to study the effect of the percentage and the length of flax fibers on the early age behavior of earth concrete. First, the experimental program is presented. Then, the results concerning the evolution of the horizontal plastic shrinkage, the evaporation rate and the capillary pressure are exposed. Finally, the effect of fibers on the plastic shrinkage cracking of earth concrete is investigated based on the DIC data.

2. Experimental program

2.1. Materials

2.1.1. Soil and Hydraulic binders

Earth concrete mixture used in this study is based on an artificial soil composed of 30% of bentonite clay (75% of Smectite, 15% of Illite and 10% of Kaolinite) and 70% of sand. This clay was supplied by Lafaure quarry. Its characteristics are presented in Table 1. This clay has been chosen in order to taken into account variability of the soil on site considering unfavorable properties. In addition, as the objective of this work is to study the efficiency of fibers in the reduction of shrinkage, choosing a clay responsible of a higher shrinkage rate was convenient. In fact, this clay is known for its high swelling properties. It attracts water into the voids due to suction, causing a change in the voids volume. During hydration, the confined layer of dry bentonite changes into a dense monolithic mass with no discernable individual particles [44]. An artificial soil has been used to limit the variability of natural soil and thus to better distinguish the effect of flax fibers. The artificial soil has been stabilized with 3% of natural hydraulic lime (NHL5/ EN 459-1 [45]) and 8% of cement (CEM 1, 52.5 N PM-CP2 / EN197-1 [46]) based on the clay and sand mixture mass. Those percentages have been fixed according to other studies presented in the literature that showed that 2% to 4% of lime are sufficient to stabilize the soil [15, 47], and the optimal percentage of cement to ensure a sufficient strength for the earth concrete is 8% [48]. The mineralogical composition of cement is presented in Table 2. The pure Portland cement CEM 1 composed mainly of clinker is chosen to prevent the effect of any additional component, present in other types of cement, on the mixture.

Table 1. Bentonite clay properties

Natural water content	Liquid limit	Plastic limit
6.7%	84.6%	29.2%

Table 2. Mineralogical composition of cement

Main components	C_3S	C_2S	C_4AF	C_3A	SO_3, NA_2O, S^-
Percentages (%)	65	12	6	12	>5

Figure 1 presents the grain size distribution of the sand, the bentonite and their mixture that constitute the artificial soil. This analysis has been carried out by sieving according to the standard (XP P 94-041 [49]) for particles having a diameter greater than 0.08 mm and by sedimentation according to the standard (NF P94-057 [50]) for fine particles (<0.08 mm).

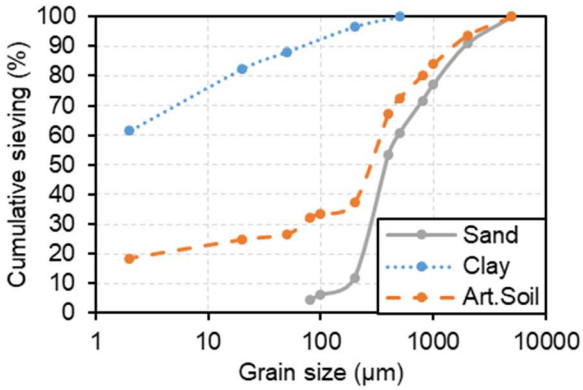

Figure 1. Grain size distribution of sand, clay and the resultant artificial soil

2.1.2. Flax fibers

Flax fibers are natural fibers, bio-renewable, recyclable and biodegradable. The fibers were cut at constant lengths of 12, 24 and 50 mm and their diameter is equal to 14.66 µm ±2.95 [49] (Figure 2). These fibers are rich in cellulose, more than 60% of their constitution, which gives them good tensile strength properties [52]. However, one of the main problems of natural fibers is their hydrophilicity propertie which is linked to their high-water absorption that can have an important effect on the workability and on the behavior of earth concrete at early age. In addition, the presence of water or moisture in the pore system of natural fibers decreases their strength and stiffness and modifies their chemical composition [53, 54]. The fibers used in this study were not treated in order to keep these

materials natural and easy to use. In fact, different types of treatment for natural fibers have been tested in the literature (Alkaline treatment, acetylation, hydrothermal treatment, water repellent coating, ect…) with the aim to improve their properties and the adhesion with earth concrete matrix. However, each treatment can enhance some properties and at the same time has negative effects on the others [9].

The absorption test has been also conducted based on the experimental protocol developed by the RILEM TC 236-BBM group [55]. The coefficient of absorption has been determined for the three fibers lengths used in this study (Figure 3). The obtained results are in the same range of those found in [51]. The coefficient of absorption increased with an important rate in the first few minutes due to the high specific surface area of these fibers. The absorption coefficient stabilizes after approximately 60 minutes. A slight difference has been observed between the three lengths of flax fibers used with an increase of the absorption coefficient for the smaller length which may be explained by the increase of their specific surface area. The water added in the mixtures has been adjusted according to this value.

The adsorption/desorption curves (NF EN ISO 12571) [56] have been also plotted (Figure 4). The results show that the behavior of fibers with three different lengths is almost the same. The quantity of water loss during desorption is not the same as that absorbed at the same moisture. This hysteresis between adsorption and desorption curves is related to the content of lignin presented in the fibers and to the microporous structure of fibers that influences the retention of the water [57, 58].

Figure 2. Different lengths of flax fibers

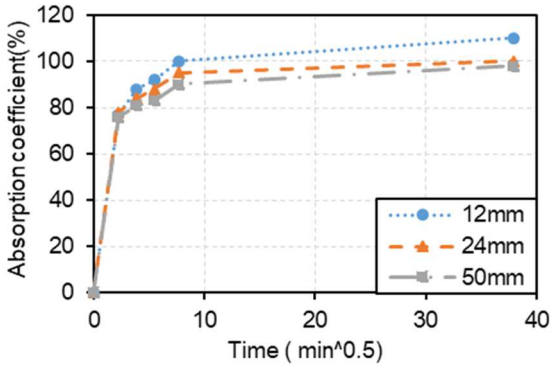

178

179 **Figure 3.** Evolution of the absorption coefficient in function of time for fibers with a length of 12, 24

180 and 50 mm

181

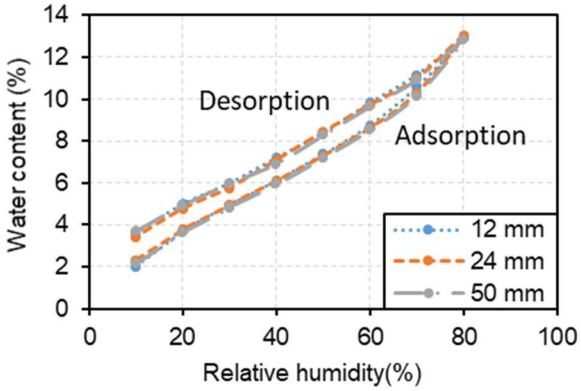

182

183 **Figure 4.** Variation of water content in fonction of the relative humidity for fibers with a length of

184 12, 24 and 50 mm

185

186 *2.1.3. Mixtures*

187 Seven mixtures have been tested by varying the percentage (0, 0.3 and 0.6%) and the length (12, 24

188 and 50 mm) of fibers. Clay and sand have been mixed first during 3 minutes to ensure a certain

189 homogeneity of the artificial soil. Then, the lime and the cement have been added to the dry mixture

190 and mixed during 2 minutes. The water and the superplasticizer have been then added and mixed for

191 3 minutes. The superplasticizer Tempo 10 has been used in this study due to its efficiency as a water

192 reducer admixture in earth concrete [30]. Finally, the fibers have been progressively added and mixed

193 during 3 minutes. The mixtures have been named by presenting the % of fibers followed by the

length of fibers. For example, SA03F12 represents the formulation containing 0.3% of flax fibers with a length of 12 mm. Table 3 presents the components of these mixtures. The quantity of added fibers is subtracted from the artificial soil mass to keep an equivalent solid mass. The effective water to binder ratio has been kept constant and equal to 0.45. Additional water has been added to take into account the water absorbed by flax fibers.

The slump (EN 12350-2) [59] and air entrained (EN 12350-7) [60] tests have been conducted on fresh earth concrete for each mixture.

Table 3. Mixtures components and composition

Components (kg/m^3)	Sand	Bentonite	Cement	Lime	Effective water	Total water	Super-plasticizer	Flax fibers
SA0F0	931	405	152	34.2	83.8	367	1.6	0
SA03F12/24/50	929	401	152	34.2	83.8	370	1.6	5.7
SA06F12/24/50	925	399	152	34.2	83.8	375	1.6	11.4

3. Methods

3.1. Compressive strength test

Unconfined compressive tests have been conducted using an electromechanical machine with a capacity of 100 kN and a constant loading displacement rate of 0.6 mm/min. This test has been realized on cubic specimens of 10×10×10 cm^3 at the age of 7, 28 and 180 days. These specimens have been cured in a climatic chamber with a relative humidity of 80-95%.

3.2. Horizontal plastic shrinkage

The horizontal free plastic shrinkage has been measured on fresh earth concrete samples placed in a prismatic teflon mold of 7 x 7 x 28 cm^3 using two LVDT sensors with a precision of 3 µm (Figure 5). Tests have been carried out in an air-conditioned room at 20 ± 1 °C and a RH of 60 ± 2 % [34]. This test has been realized under sealed and drying conditions. Under sealed condition, the top of the specimen has been covered by a plastic sheet to prevent the drying of earth concrete. The weight loss,

the temperature and the capillary pressure have been also measured in parallel. Two thermocouples have been used to measure the temperature evolution. The first has been inserted in the middle of concrete specimen immediately after casting and the second has been used to monitor the external temperature. These thermocouples were connected to a data-logger to record the temperature after concrete casting. The weight loss of earth concrete during drying has been also monitored after casting by measuring continuously the weight of a concrete sample with a height of 70 mm. During drying, the relative humidity of earth concrete decreases which induces a drop-in pressure in the liquid phase. A meniscus is thus formed at the interface with the gaseous phase generating a capillary pressure. The capillary pressure was measured using a tensiometric sensor placed in the middle of a cylindrical mold (with a diameter of 11 cm and a height of 7 cm). The sensor pores have been saturated in water before being integrated in concrete. The data acquisition of all these measurements starts after 1 hour of adding water to the mixture and lasts for 24 hours.

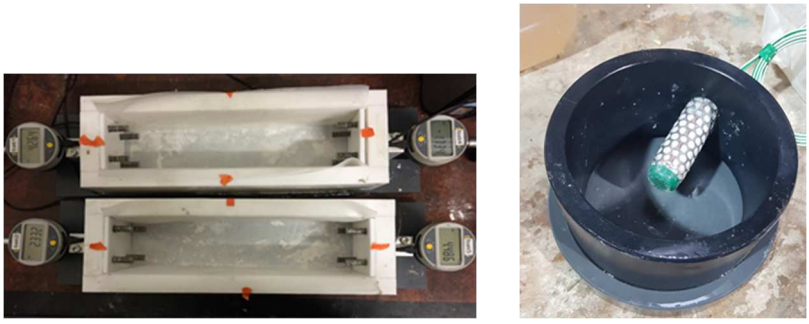

Figure 5. Plastic shrinkage and capillary pressure measurement devices

3.3.Plastic shrinkage cracking

The susceptibility of earth concrete to plastic shrinkage cracking has been studied according to ASTM C1579-13 [61]. The test presented in figure 6 includes a mold with a large metal notch in the middle, which acts as a stress riser and thus responsible of crack initiation due to restrained concrete. The other two smaller metal notches on the sides serve as internal retainers. The molds were filled with concrete to the top and the surface finishing is done using a darby tool.

The tests have been conducted in a climate-controlled room with a constant temperature of 34 ± 1 °C and a relative humidity of 33 ± 6%. The wind velocity must be sufficient to obtain a minimum evaporation rate of (1 kg/(m^2.h)). For this reason, a fan with a wind speed of 6 ± 1 m/s has been used and directed to the surface of the specimens to obtain the desired evaporation.

The tests have been monitored with the DIC technique during 24 hours after casting in order to study the effect of the percentage and length of fibers on the behavior of earth concrete at early age. A speckle pattern of black and white paint has been sprayed onto the surface of the specimen to improve the displacement resolution. Images have been captured using a digital camera with a resolution of 2560 × 2048 pixels. Two lamps have been used to improve the luminosity of the images. Each pixel stores a grey scale value ranging from 0 to 255 according to the intensity of the reflected light by the surface of the target. Images have been taken at a rate of one image each 8 seconds during the test with a resolution of 0.17 mm per pixel. The images have been treated later using the commercial software Vic 2D.

To calculate the deformation on the surface of the specimens, the grey patterns of pixel subsets on the reference image have been compared with those of the deformed specimen. The displacement result expressed in the center point of the subset is an average of the displacement of the pixels inside the subset. The crack width and area have been also measured using image J software.

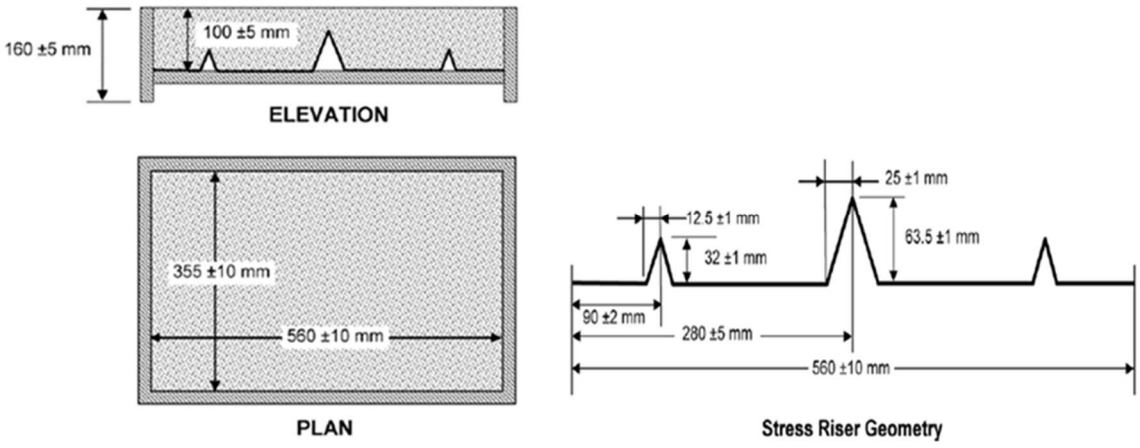

Figure 6. Specimen and stress riser geometry

3.4. Mercury intrusion porosimetry

The effect of flax fibers on the pore size distribution of earth concrete with and without fibers after 28 days has been also evaluated using mercury intrusion porosimetry (MIP). In this test, pressure was used to press non-wetting liquid mercury into the pores of earth concrete. These tests have been realized on a little cube of 1.4 cm ± 0.1 of earth concrete with a mass of almost 6 g at the age of 28 days. MIP measurements were performed with an Autopore III 9420 from Micrometrics®. The amount of pressure needed to force the mercury into pores of certain sizes is inversely proportional to the pore size. The range of low and high pressure was respectively 0.0007 and 420.5 Mpa. The measurements have been recorded and used to draw the pore volume against the pore radius.

4. Results and Discussions

4.1. Properties of fresh concrete

The slump test shows that adding fibers affects highly the workability of earth concrete (Figure 7). This is due to the high specific surface, the small diameter and the hydrophilic property of these fibers. The maneuverability or slump of earth concrete decreases with the percentage of fibers content. However, the length of flax fibers did not present a significant influence on concrete workability, which may be due to the high flexibility of flax fibers. Even though, a small reduction of the slump value has been observed for the longest fibers (50 mm). Note that in some cases, long fibers provoked segregation during mixing of earth concrete. In addition, the air content increased with the incorporation of flax fibers in earth concrete especially for longer fibers.

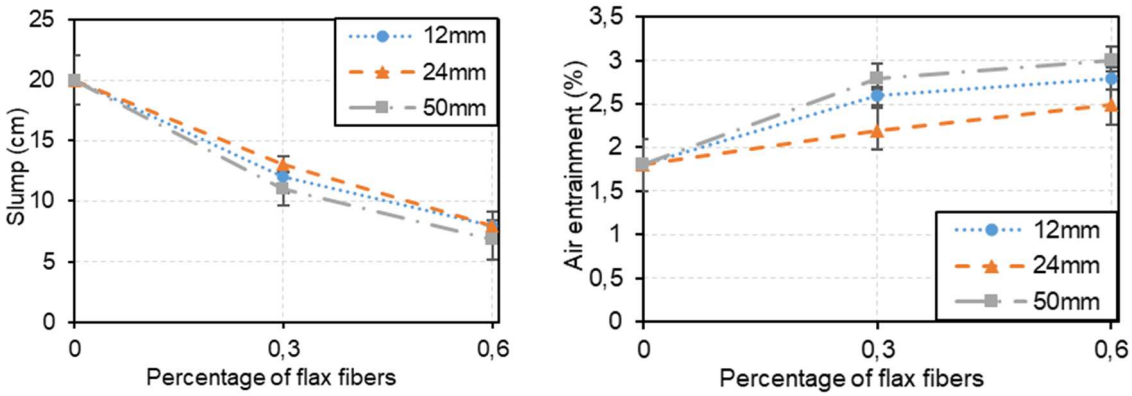

279

280 **Figure 7.** Slump and air content of fresh earth concrete with different percentages and lengths of

281 flax fibers

282

283 ### 4.2. Compressive strength

284 Three specimens have been tested for each mixture to study the repeatability. Figure 8 presents the
285 maximum compressive strength of the different mixtures at 7, 28 and 180 days. At the 7th and the
286 28th days, the compressive strength increased with the addition of fibers and is more significant with
287 the addition of 0.6% of flax fibers [9]. This can be associated to the good adhesion between fibers
288 and earth concrete matrix that prevented the spreading of cracks and improved the mechanical
289 properties [9]. The length of fibers did not show a significant effect on the compressive strength.
290 Note that, no generalized conclusion can be made on the effect of natural fibers on the compression
291 strength. The results depend on the type and the percentage of the used soil and fibers, in addition to
292 the testing method and many other criteria [9]. For example, while the addition of 20% of oat straw
293 reduced the compression strength, the addition of the same percentage of typha fiber-wool increased
294 it [62].

295

296 The compressive strength increases significantly even after 28 days and doubled at 180 days, which
297 may be due to pozzolanic and hydration reactions related to lime and cement. These reactions
298 increase the cohesive force between the clay particles and thus the mechanical properties of earth
299 concrete [13, 20, 28]. Note that, the clay mineralogy has an important influence on the physical and
300 mechanical properties of earth concrete [63].

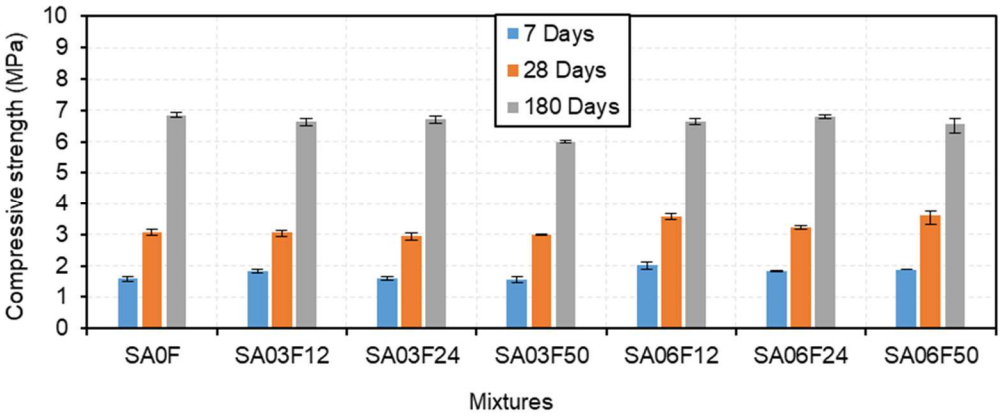

Figure 8. Compressive strength of earth concrete with different percentages and lengths of flax fibers at 7, 28 and 180 days of curing

Figure 9 presents the fracture behavior of earth concrete specimens with different percentages of fibers (0%, 0.3% and 0.6%). A brittle behavior has been observed for SA0F, accompanied with the propagation of a large crack from the bottom to the top of the specimen during the compressive test. However, for specimens containing fibers, a multi cracking has been observed with a crack length way smaller than that obtained with SA0F. The same observation has been found with [28, 64]. Thus, the addition of flax fibers improved greatly the compressibility, the fracture energy and the ductility of earth concrete [9]. This is due to the bridging effect of the fibers and to their high compressibility [9].

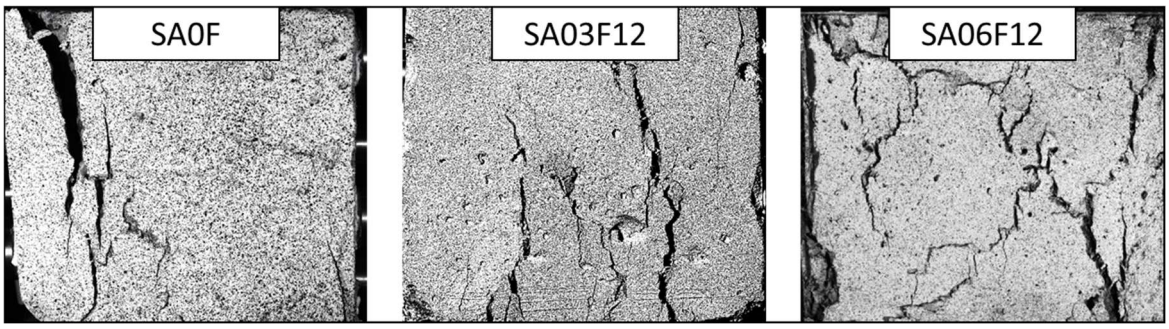

317 **Figure 9.** Fracture behavior of earth concrete specimens for SA0F, SA03F12 and SA06F12 mixtures
318 at the age of 28 days
319

320 ## 4.3.Plastic shrinkage results

321 Plastic shrinkage tests started one hour after the contact between the water and the mixture of solid
322 materials. The horizontal shrinkage was calculated as the mean value of the data collected from the
323 displacement of the two sensors. Figure 10 shows the crossed curves of the early age/drying
324 shrinkage development, the weight loss and the capillary pressure for SA0F. The weight loss is
325 expressed in kg/m^2 and is multiplied by a coefficient of 30 to be compatible with the secondary axis
326 of the capillary pressure.
327 The maximum plastic shrinkage value of earth concrete is much higher than the shrinkage of ordinary
328 concrete due to the presence of the clay [34, 65, 66].
329 Based on the analysis of the early age shrinkage curves, four phases can be distinguished. In the first
330 phase, plastic shrinkage starts to develop almost immediately after casting with a small rate and a low
331 capillarity at the surface of concrete. This indicates a very thin layer of bleeding water on the surface
332 which may be due to the absorption of water by fine particles and fibers. In the second phase,
333 shrinkage increases with an important rate, which may be related to the increase of the capillary
334 pressure due to the evaporation and the consumption of water by the hydration reactions. The
335 increase of the capillary pressure indicates that the meniscus started to appear in the pores of the
336 mixture near the sensor placed in the middle of the sample. During the third phase, the rate of plastic
337 shrinkage started to decrease until reaching its stabilization where the plastic shrinkage attends its
338 limit and the volumetric contraction stops. This occurs when the solid skeleton of earth concrete
339 stiffens enough due to the different hydration reactions and can resist to the capillary pressure. The
340 rate of the weight loss decreases with the different stages to attend almost 1% of evaporation (2
341 kg/m^2) after 24 h of concrete casting.
342

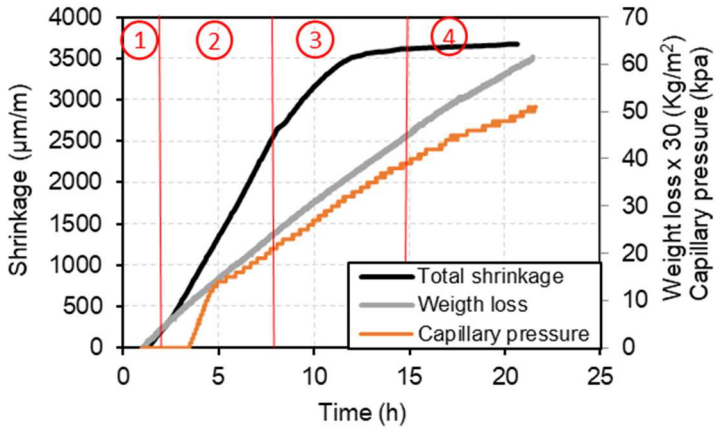

343

344 **Figure 10.** Development of plastic shrinkage, weight loss and capillary pressure for SA0F

345

346 Figure 11 shows the comparison between the horizontal early age shrinkage development for SA0F,
347 SA03F12 and SA06F12 mixtures. The rate of the development of the shrinkage has been also plotted.
348 The results show that the rate of development of plastic shrinkage for SA0F is much higher than that
349 for specimens with fibers. In the first 7.5 h for SA0F, 6.7 h for SA03F12 and 6.2 h for SA06F12, the
350 velocity of the deformation was high and almost constant. However, the rate of displacement
351 decreases with the percentage of fibers. Then, the rate of deformation decreases to reach zero. For
352 SA0F, this decrease is slow and progressive before it vanishes after 14 hours. However, the rate of
353 deformation for the mixtures with 0.3 and 0.6% of fibers decreases quickly and stabilizes after 10
354 hours.

355

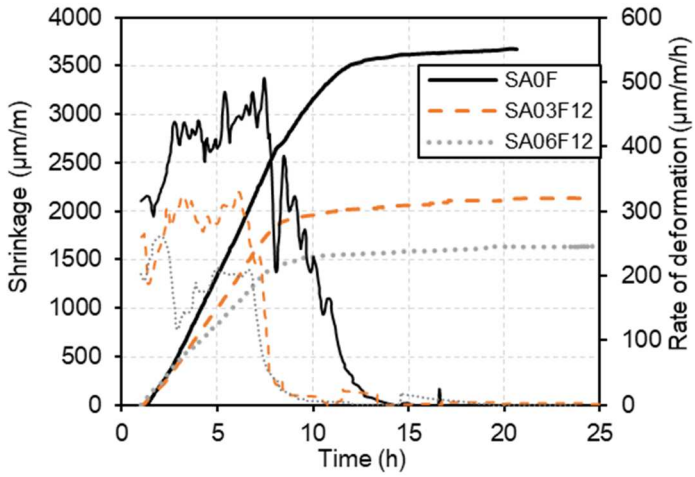

356

Figure 11. Evolution of the plastic shrinkage and the deformation rate for SA0F, SA03F12 and SA06F12 mixtures

Figure 12 and 13 present the evolution of early age plastic and autogenous shrinkage for all the mixtures with 0, 0.3 and 0.6% of fibers and considering the three lengths of 12, 24 and 50 mm. The rate and amplitude of autogenous shrinkage is low with a maximum value of 500 µm/m for SA0F. This may be due to different hydration reactions of cement and lime or chemical shrinkage in addition to self-desiccation shrinkage, which occurs in moisture-sealed conditions as water is internally removed from the capillary pores by chemical combination during hydration.

The plastic shrinkage started directly after casting for all the mixtures under drying. The plastic shrinkage is reduced 2 to 2.4 times with the addition of 0.3% and 0.6% of fibers respectively compared to SA0F.

All the mixtures with fibers attend the plastic shrinkage stabilization at the same age earlier then SA0F. The effect of fiber lengths is more pronounced for the formulation with 0.3% of fibers. In fact, the increase of fiber lengths leads to the reduction of the rate and amplitude of plastic shrinkage, which may be due to the large surface that can be occupied by each fiber holding back the particles of concrete together.

Figure 13 presents the average maximum value of plastic shrinkage for the different mixtures considering the repeatability of the results. Plastic shrinkage decreases with an important rate with the addition of fibers. In addition, it decreases slightly with the percentage and length of fibers.

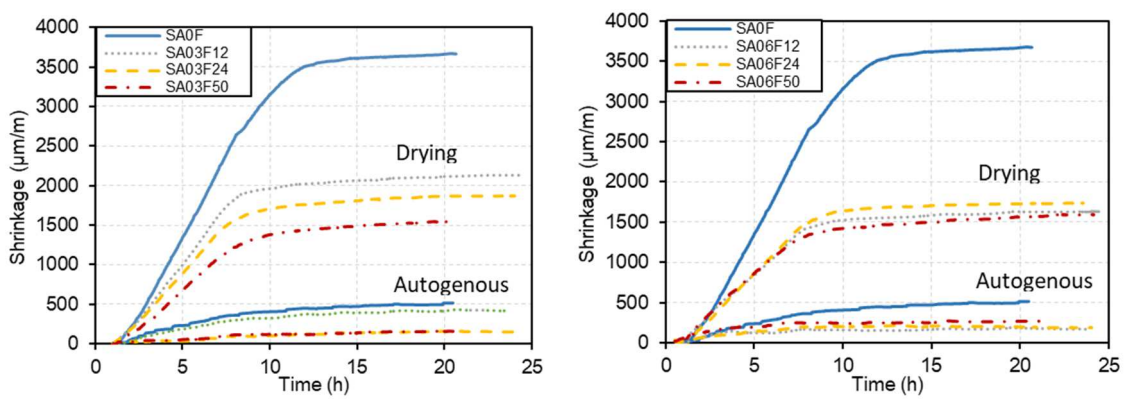

Figure 12. Evolution of plastic and autogenous shrinkage for mixtures without and with 0.3% a) and 0.6% b) of fibers with different lengths

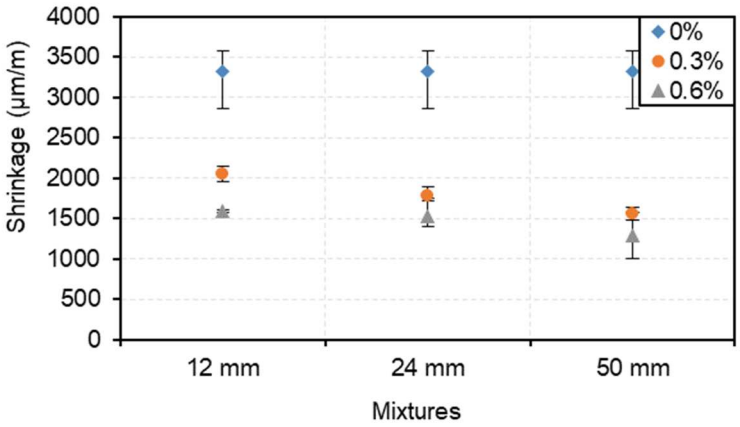

Figure 13. Maximum plastic shrinkage values of earth concrete specimens with different percentages and lengths of flax fibers

The evolution of temperature for earth concrete samples is presented in Figure 14. The temperature varies slightly between 18.5°C and 21°C. The temperature decreases in function of time with a higher rate for SA0F compared to the mixtures containing fibers until it stabilizes. It is also interesting to note that the temperature gradient of the specimens was not very significant. The temperature evolution of earth concrete is different from that of ordinary concrete as no temperature peak related to the exothermic hydration reactions is observed which may due to the small quantity of added cement [67, 68].

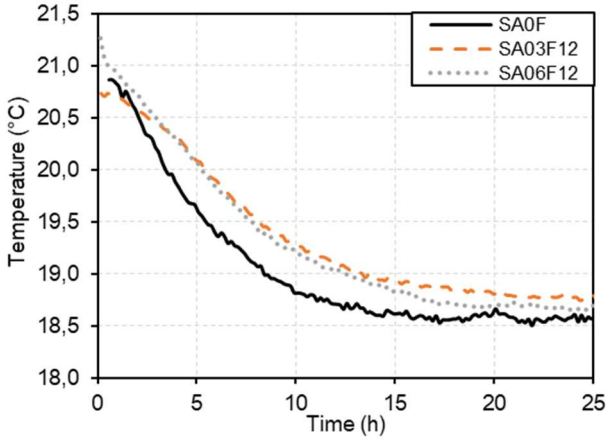

394

395 **Figure 14.** Evolution of the ambient and concrete temperature for the mixtures SA0F, SA03F12 and
396 SA06F12 at early age

397

398 The evaporation rate for the mixtures with different lengths and percentages of fibers is presented in
399 figure 15. The results show that there is no clear tendency of the evolution of the evaporation rate in
400 function of different percentages and lengths of fibers. Note that the evaporation rate is considered
401 low according to ACI 305.R-99 [69]. Many research in the literature showed also a contradiction
402 between the evolution of the evaporation rate at early age for concrete with and without fibers [33].
403 The observed variability can be related to many factors such as the distribution of fibers in concrete,
404 its surface finishing, the number of interconnected capillary voids that allows water to rise easily, in
405 addition to the hydrophilicity properties of fibers that may be responsible of the water retention and
406 the reduction of the segregation and thus the quantity of bleeding water [33, 37].

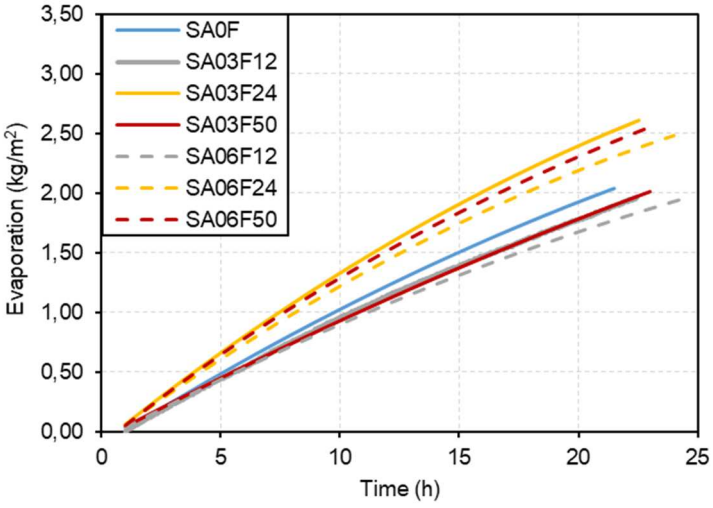

407

408 **Figure 15.** Evolution of the weight loss for all the mixtures at early age

Figure 16 presents the evolution of the capillary pressure during the first 24 hours. The capillary pressure is directly related to the pore distribution in the matrix. According to Laplace's equation, the capillary pressure increases when the pore radius decreases:

$$P = (-(2\gamma)/R).\cos\theta \qquad \text{Equation 1}$$

where P is the pressure in the pore liquid, θ is the wetting angle, R is radius of the pore containing the meniscus and γ is the surface tension of the liquid/water.

The capillary pressure was delayed for all the formulation for few hours; 2.5 hours for the formulations containing fibers and 3.5 hours for SA0F. This is related to the transfer properties and kinetic of drying that control the saturation of concrete pores system along the height of the specimens as the sensor is placed in the middle of the mold [35]. For the mixtures containing fibers, the capillary pressure developed earlier than SA0F. This may be due to the low amount of bleeding water with mixtures containing fibers and different transfer properties related to the percentage and distribution of pores that can affect the value of the capillary pressure in concrete in addition to the absorption of water by the different materials presented in concrete as clay and fibers.

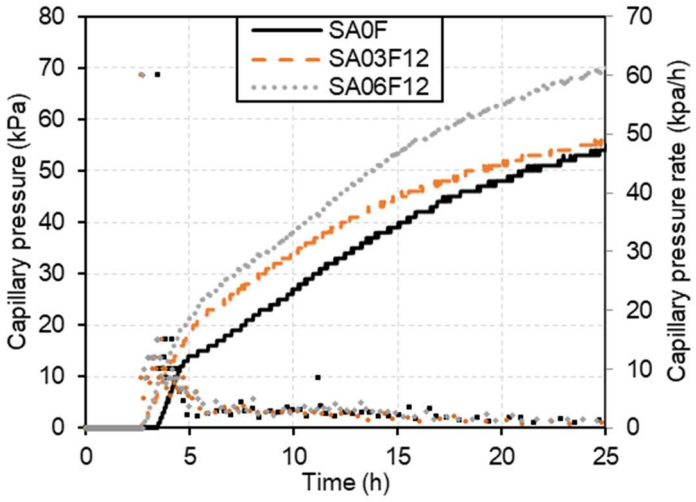

Figure 16. Evolution of the capillary pressure and its rate for SA0F, SA03F12 and SA06F12 mixtures

4.4.Results from mercury intrusion porosimetry

In order to have a better understanding of those differences between the mixtures with and without fibers, the effect of fibers on the pore size distribution has been evaluated using a high-pressure mercury intrusion porosimeter. Figure 17 shows the evolution of the increment pore volume with respect to the logarithm of the pore radius in function of the pore radius r for SA0F, SA03F24 and SA06F24. The results show that the total porosity is equal to 35% for the fiber-free formulations, 36% for the SA03F24 and 40% for the SA06F24 formulations. The pore distribution range varies between 0.005 µm to 70 µm. From a dynamic point of view, the experiments take place from right to left i.e, large access radii (Washburn's law) towards small access radii. The distribution is largely dominated by a main mode centered at 1 µm for the three mixtures. Two secondary modes have been also observed at 0.05 µm on small pore side and 8 µm on large pore side. The results show that the volume of small pores (smaller than 0.1 µm) is slightly higher for SA06F24, which explains the higher capillary pressure. The volume of the pores with a diameter between 0.1 and 5 µm is highest for SA03F24. However, the volume of pores with a diameter larger than 5 µm is bigger for specimens with 0.6% of fibers, which may be due to the effect of fibers distribution in the specimen in large quantities. The differences between the total porosity and the pore distributions may explain the capillary pressure development delay and the different evaporation rate observed with the different mixtures and are responsible of the modification of mechanical and transfer properties of earth concrete.

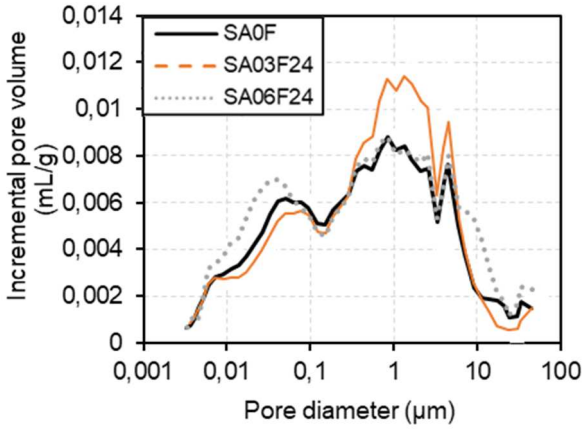

Figure 17. Pore size distribution for SA0F, SA03F24 and SA06F12

4.5.Plastic shrinkage cracking

Plastic shrinkage cracking tests started one hour after mixing earth concrete. The images taken during the test (first 24 hours) are used to compute the displacement and the strain fields with the DIC technique. Figure 18 presents the evolution of the strain field in the x-direction (exx) for the SA0F. The crack initiated after almost 3.8 hours of casting the earth concrete and spreaded in 20 min along the large notch in the middle of the mold to form a continuous macro-crack. Figure 19 presents the evolution of the strain along the x-axis of the mold. The strain increases in the area near the notch. The tensile strength is at its maximum value near the cracking area for the formulation SA0F where strain values are red. The crack occurred due to the restrained shrinkage of earth concrete, which generates tensile stresses responsible of cracking when they exceeded the maximum stress capacity of concrete. The image j software has been used to characterize the crack that reached an area of 434 ± 55 mm^2 and a width of 1.7 ± 0.2 mm after 24 hours.

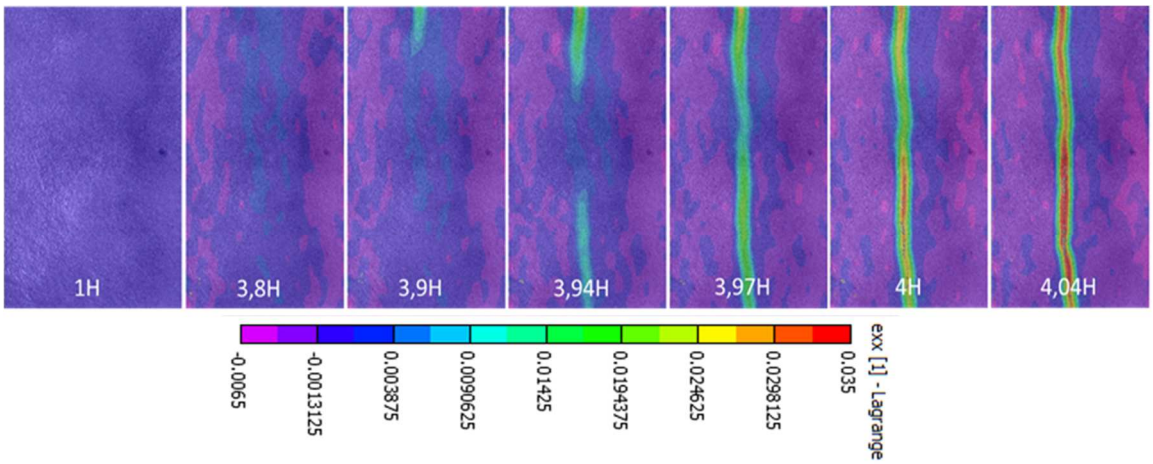

Figure 18. Evolution of the strain field for SAF in function of time

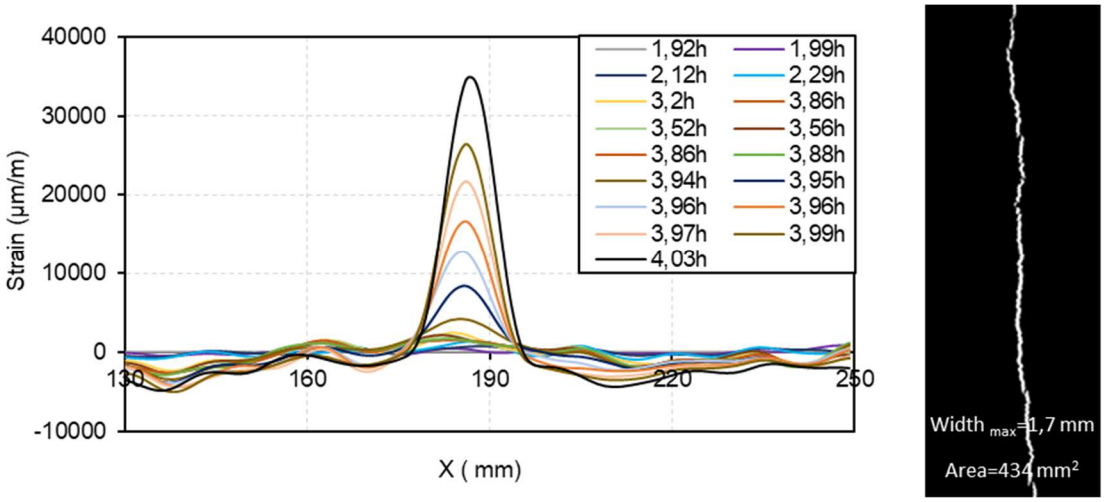

Figure 19. a) Evolution of the strain field in function of the x axis in function of time (per hour) measured in the middle of the mold b) Crack area and width for SA0F

For the formulations containing flax fibers with a length of 12, 24 and 50 mm, no macro-cracks have been observed during the first 24 hours after casting. Figure 20 shows the strain fields for the mixtures SA06F12, SA06F24 and SA06F50. The results show that the zone of concentration of strain fields is larger than the one obtained with SA0F. In addition, the strain values were significantly less important indicating the reduction of plastic shrinkage cracking due concrete reinforcement with flax fibers. In fact, flax fibers increase the early age tensile strength [39] which make it more difficult to reach the strength of concrete at this age [31]. New bridging forces are developed due to the presence of fibers, which prevent crack propagation [37, 70]. In addition, the presence of flax fibers tends to reduce the quantity of bleeding water, which enhance the concrete stiffness at its early age [9].

In addition, the DIC results showed that the strain concentration localized above the stress riser using the shorter length of fibers (12 mm) is higher than that using the longest length of flax fibers (50 mm). This may be due to the larger space occupied by the longest fibers, which is responsible of stress redistribution and thus a decrease of the maximum strain values. In fact, longer fibers allow obtaining a sufficient stress transfer and a reduction of the stress concentration across the crack position [33, 71, 72].

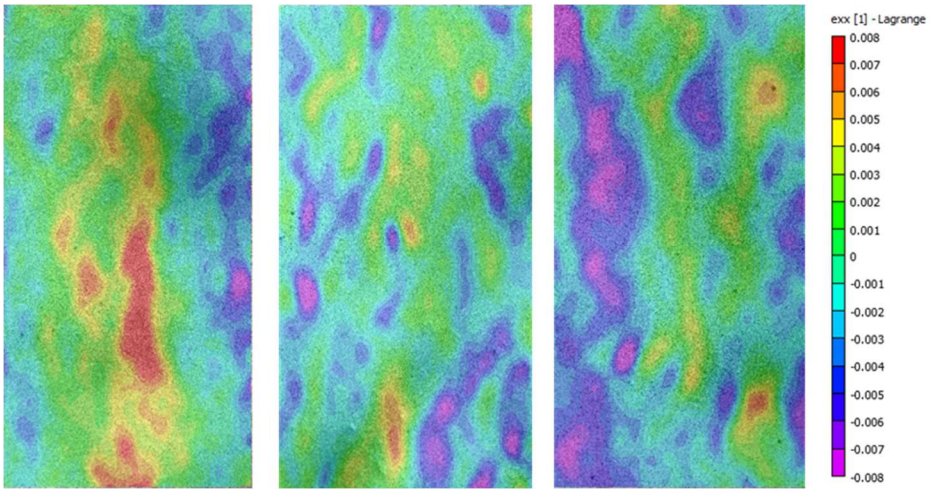

Figure 20. Evolution of the strain field for SA06F12, SA06F24 and SA06F50 mixtures 24 hours after casting

5. Conclusion

The earth concrete studied in this article is a building material that can be created on site using excavated soil and local materials in regions with few natural resources for different applications in the construction field. It can be used to construct load bearing walls or slabs for small structures or for non-structural elements and plasters with a lower thickness. In addition to its environmental and ecological properties, the use of this material in building envelope can provide a certain insulation level and thermal inertia. The effect of incorporation of flax fibers with different lengths and percentages on the early age behavior of earth concrete has been studied. The evolution of plastic shrinkage has been studied in parallel to the evaporation and the capillary pressure during the first 24 hours after casting of earth concrete. The stain and displacement fields of the restrained earth concrete specimens with and without fibers have been evaluated using DIC technique. The main conclusions of this study are:

- Flax fibers increase slightly the compressive strength at 28 days of earth concrete and enhance the ductility by generating a multi–cracking propagation in the specimen.
- The horizontal plastic shrinkage of earth concrete decreases with the increase of the percentage and length of flax fibers.
- The addition of fibers reduces the cracking risk of restrained earth concrete at the early age. No macro-cracks have been observed with mixtures containing flax fibers due to the

reduction of stress concentration above the stress riser of the mold. An increase in the strain distribution has been also observed at the specimen surface with the increase of the fiber length indicating a better stress transfer.

Additional studies will be realized in the future in order to study the effect of these fibers on the fracture behavior, the durability and the hydrothermal properties of earth concrete.

References

[1] H. Dahlbo, J. Bachér, K. Lähtinen, T. Jouttijärvi, P. Suoheimo, T. Mattila, S. Sironen, T. Myllymaa, K. Saramäki, Construction and demolition waste management – a holistic evaluation of environmental performance, J. Clean. Prod. 107 (2015) 333-341, https://doi.org/10.1016/j.jclepro.2015.02.073.

[2] C. Llatas, A model for quantifying construction waste in projects according to the European waste list, Waste Manag. 31 (6) (2011) 1261-1276, https://doi.org/10.1016/j.wasman.2011.01.023.

[3] L. Perez-Lombard, J. Ortiz, C. Pout, A review on buildings energy consumption information, Energy Build. 40 (3) (2008) 394–398, https://doi.org/10.1016/j.enbuild.2007.03.007.

[4] H. Van Damme, H. Houben, Earth concrete. Stabilization revisited, Cem. Concr. Res. 114 (2017) 90–102 , https://doi.org/10.1016/j.cemconres.2017.02.035.

[5] F. Pacheco-Torgal, S. Jalali, Earth construction: lessons from the past for future eco-efficient construction, Constr. Build. Mater. 29 (2012) 512–519, https://doi.org/10.1016/j.conbuildmat.2011.10.054.

[6] L. Eloundou, Earthen Architecture in today's World, in Proceedings of the UNESCO International Colloquium on the Conservation of World Heritage Earthen Architecture, Paris UNESCO. 36 (2013), http://whc.unesco.org/document/126549

[7] C. Williams, S. Goodhew, R. Griffiths, L. Watson, The feasibility of earth block masonry for building sustainable walling. United Kingdom. J. Build. Apprais, 6 (2) (2010) 99–108, https://doi.org/10.1057/jba.2010.15.

534 [8] M.S. Zami, A. Lee, Economic benefits of contemporary earth construction in low-cost urban
535 housing. State-of-the-art review, J. Build. Apprais. 5 (3) (2010), 259–271,
536 https://doi.org/10.1057/jba.2009.32.
537 [9] A. Laborel-Préneron, J.E. Aubert, C. Magniont, C. Tribout, A. Bertron, Plant aggregates and
538 fibers in earth construction materials: A review, Constr. Build. Mater. 111 (2016) 719–734,
539 https://doi.org/10.1016/j.conbuildmat.2016.02.119.
540 [10] S.M. Rao, P. Shivananda, Role of curing temperature in progress of lime-soil reactions,
541 Geotech. Geol. Eng. 23 (2005) 79-85, https://doi.org/10.1007/s10706-003-3157-5.
542 [11] F. Sariosseiri, B. Muhunthan, Effect of cement treatment on geotechnical properties of some
543 Washington State soils, Eng. Geol. 104 (1–2) (2009) 119–125,
544 https://doi.org/10.1016/j.enggeo.2008.09.003.
545 [12] B. Taallah, A. Guettala, The mechanical and physical properties of compressed earth block
546 stabilized with lime and filled with untreated and alkali-treated date palm fibers, Constr. Build.
547 Mater. 104 (2016) 52–62, https://doi.org/10.1016/j.conbuildmat.2015.12.007.
548 [13] J.L. Eades, R.E. Grim, Reaction of hydrated lime with pure clay minerals in soil stabilization.
549 Highway Research Board, (262) (1960) 51-63.
550 [14] F.G. Bell, Lime stabisation of clay soils, Bulletin of the International Association of
551 Engineering Geology. 39 (1) (1989) 67–74.
552 [15] F.G. Bell, Lime stabilization of clay minerals and soils, Eng. Geol. 42 (1996) 223–237,
553 https://doi.org/10.1016/0013-7952(96)00028-2.
554 [16] K. Lemaire, D. Deneele, S. Bonnet, M. Legret, Effects of lime and cement treatment on the
555 physicochemical, microstructural and mechanical characteristics of a plastic silt, Eng. Geol. 166
556 (2013) 255–261, https://doi.org/10.1016/j.enggeo.2013.09.012 .
557 [17] S. Andavan, Vamsi Krishna Pagadala, A study on soil stabilization by addition of fly ash and
558 lime, Mater. Today Proc. 22 (3) (2020) 1125-1129, https://doi.org/10.1016/j.matpr.2019.11.323.
559 [18] J.L Parracha, A. Santos, M. Cotrim, P.Faria, Mineralogical and microstructural
560 characterisation of rammed earth and earthen mortars from 12th century Paderne Castle, J. Cult.
561 Herit. 42, (2020) 226-239, https://doi.org/10.1016/j.culher.2019.07.021.

562 [19] D.I. Boardman, S. Glendinning, C.D.F. Rogers, Development of stabilisation and
563 solidification in lime–clay mixes, Géothechnique. 51 (6) (2001) 533–543,
564 https://doi.org/10.1680/geot.2001.51.6.533.
565 [20] S. Diamond, J.L. White, W.L. Dolch, Transformation of Clay Minerals by Calcium Hydroxide
566 Attack, Clays Clay Miner. 12 (1) (1963) 359–379.
567 [21] J. Locat, M.A. Berube, M. Choquette, Laboratory investigations on the lime stabilizations of
568 sensitive clays: shear strength development, Can Geotech J. 27 (3) (1990) 294–304.
569 [22] B. Le Runigo, V. Ferber, Y. J. Cui, O. Cuisinier, D. Deneele, Performance of lime-treated silty
570 soil under long-term hydraulic conditions, Eng. Geol. 118 (1–2) (2011) 20–28,
571 https://doi.org/10.1016/j.enggeo.2010.12.002 .
572 [23] B.V. Reddy, P. Kumar, Embodied energy in cement stabilised rammed earth walls, Energy
573 Build. 42 (3) (2010) 380-385, https://doi.org/10.1016/j.enbuild.2009.10.005.
574 [24] A. Kumar, D. Gupta, Behavior of cement-stabilized fiber-reinforced pond ash, rice husk ash–
575 soil mixtures, Geotextiles Geomembr. 44 (3) (2016) 466–474,
576 https://doi.org/10.1016/j.geotexmem.2015.07.010.
577 [25] M. Carmen, Jimenez Delgado, I. Canas Guerrero, Earth building in Spain, Constr. Build.
578 Mater. 20 (2006) 679-690, https://doi.org/10.1016/j.conbuildmat.2005.02.006.
579 [26] P. Narloch, P. Woyciechowski, J. Kotowski, I. Gawriuczenkow, E. Wójcik, The Effect of Soil
580 Mineral Composition on the Compressive Strength of Cement Stabilized Rammed Earth, Materials,
581 13 (2) (2020) 324, https://doi.org/10.3390/ma13020324.
582 [27] T. Santos, L. Nunes, P. Faria, Production of eco-efficient earth-based plasters: influence of
583 composition on physical performance and bio-susceptibility, J. Clean. Prod. 167 (2017) 55-67,
584 https://doi.org/10.1016/j.jclepro.2017.08.131.
585 [28] M. Bouhicha, F. Aouissi, S. Kenai, Performance of composite soil reinforced with barley
586 straw, Cem. Concr. Compos. 27 (5) (2005) 617–621,
587 https://doi.org/10.1016/j.cemconcomp.2004.09.013.

588 [29] J. Eid, S. Taibi, J.M. Fleureau, M. Hattab, Drying, cracks and shrinkage evolution of a natural
589 silt intended for a new earth building material: Impact of reinforcement, Constr. Build. Mater. 86
590 (2015) 120–132, https://doi.org/10.1016/j.conbuildmat.2015.03.115.
591 [30] J.M. Kanema, J. Eid, S. Taibi, Shrinkage of earth concrete amended with recycled aggregates
592 and superplasticizer: Impact on mechanical properties and cracks, Mater. Des. 109 (2016) 378–389,
593 https://doi.org/10.1016/j.matdes.2016.07.025.
594 [31] J. Branston, S. Das, S.Y. Kenno, C. Taylor, Influence of basalt fibres on free and restrained
595 plastic shrinkage, Cem. Concr. Compos. 74 (2016) 182–190,
596 https://doi.org/10.1016/j.cemconcomp.2016.10.004.
597 [32] V. Slowik, M. Schmidt, R. Fritzsch, Capillary pressure in fresh cement-based materials and
598 identification of the air entry value, Cem. Concr. Compos. 30 (7) (2008) 557–565,
599 https://doi.org/10.1016/j.cemconcomp.2008.03.002.
600 [33] I.M.G. Bertelsen, L.M. Ottosen, G. Fischer, Influence of fibre characteristics on plastic
601 shrinkage cracking in cement-based materials: A review, Constr. Build. Mater. 230 (2020) 116769,
602 https://doi.org/10.1016/j.conbuildmat.2019.116769.
603 [34] J. Saliba, E. Rozière, F. Grondin, A. Loukili, Influence of shrinkage-reducing admixtures on
604 plastic and long-term shrinkage, Cem. Concr. Compos. 33 (2) (2011) 209–217,
605 https://doi.org/10.1016/j.cemconcomp.2010.10.006.
606 [35] [Sayahi 2016] Sayahi, F.; Plastic Shrinkage Cracking in Concrete, PHD thesis of Luleå
607 University of Technology, 2016, 10.3929/ETHZ-B-000249246.
608 [36] P.J. Uno, Plastic shrinkage cracking and evaporation formulas, ACI Mater. J. 95 (4) (1996)
609 365-375, https://www.concrete.org/publications/acimaterialsjournal.aspx.
610 [37] P. Soroushian, F. Mirza, A. Alhozaimy, Plastic shrinkage cracking of polypropylene fiber-
611 reinforced concrete. ACI Mater. J. 92 (5) (1995), 553-560.
612 [38] Z. Bayasi, M. Mclntyre, Application of fibrillated PP fibres for restraint of plastic shrinkage
613 cracking in Silica Fume Concrete, ACI Mater. J. 99 (4) (2002) 337-344.

614 [39] E. Boghossian, L.D. Wegner, Use of flax fibres to reduce plastic shrinkage cracking in
615 concrete, Cem. Concr. Compos. 30 (2008) 929–937,
616 https://doi.org/10.1016/j.cemconcomp.2008.09.003.
617 [40] S. Imanzadeh, A. Jarno, A. Hibouche, A. Bouarar, S. Taibi, Ductility analysis of vegetal-fiber
618 reinforced raw earth concrete by mixture design. Constr. Build. Mater. 239 (2020) 117829,
619 https://doi.org/10.1016/j.conbuildmat.2019.117829.
620 [41] C. Baley, M. Gomina, J. Breard, A. Bourmaud, P. Davies, Variability of mechanical properties
621 of flax fibres for composite reinforcement. A review, Ind. Crops Prod. 145 (2019) 111984,
622 https://doi.org/10.1016/j.indcrop.2019.111984.
623 [42] K. Ghavami, R.D. Toledo Filho, N.P. Barbosa, Behaviour of composite soil reinforced with
624 natural fibres, Cem. Concr. Compos. 21 (1999) 39–48, https://doi.org/10.1016/S0958-
625 9465(98)00033-X.
626 [43] A.E.M.K. Mohamed, Improvement of swelling clay properties using hay fibers. Constr. Build.
627 Mater. 38 (2013) 242–247, https://doi.org/10.1016/j.conbuildmat.2012.08.031.
628 [44] S. F. Diman, C. Wijeyesekera, Swelling characteristics of bentonite clay mats. The School of
629 Computing and Technology 3rd Annual Conference. (2008), http://hdl.handle.net/10552/781.
630 [45] EN (European Standards), Lime: Definitions, Specifications and Conformity criteria. EN 459-
631 1, (2015).
632 [46] EN (European Standards), Composition, Specifications and Conformity criteria of common
633 cements. NF EN197-1, (2012)
634 [47] S. Khattab, M. Al-Mukhtar, J.M. Fleureau, Long-term stability characteristics of a lime-treated
635 plastic soil. J. Mater. Civil Eng. 19 (2007) 358–366.
636 [48] C.A. Anagnostopoulos, Strength properties of an epoxy resin and cement stabilized silty clay
637 soil, Appl. Clay Sci. 114 (2015) 517–529, https://doi.org/10.1016/j.clay.2015.07.007.
638 [49] Standard AFNOR, Reconnaissance and testing - Size identification -Wet sieving method. XP
639 P94-041, (1995).
640 [50] NF (French Standards), Reconnaissance and testing - Particle size analysis - Sedimentation
641 method. NF P94-057, (1992).

642 [51] J. Page, F. Khadraoui, M. Gomina, M. Boutouil, Influence of different surface treatments on
643 the water absorption capacity of flax fibres: Rheology of fresh reinforced-mortars, mechanical
644 properties in the hardened state. Constr. Build. Mater. 199 (2019) 424-434,
645 https://doi.org/10.1016/j.conbuildmat.2018.12.042.
646 [52] J. Page, F. Khadraoui, M. Boutouil, M. Gomina, Multi-physical properties of a structural
647 concrete incorporating short flax fibers, Constr. Build. Mater. 140 (2017) 344-353,
648 https://doi.org/10.1016/j.conbuildmat.2017.02.124.
649 [53] L. Yan, N. Chouw, K. Jayaraman, Flax fibre and its composites – A review, Compos. Part B
650 Eng. 56 (2014) 296-317, https://doi.org/10.1016/j.compositesb.2013.08.014.
651 [54] U. Huner, Effect of Water Absorption on the Mechanical Properties \of Flax Fiber Reinforced
652 Epoxy Composites, ASTRJournal. 9 (26) (2015) 1-6.
653 [55] S. Amziane, F. Collet, M. Lawrence, C. Magniont, V. Picandet, M. Sonebi, Recommendation
654 of the RILEM TC 236-BBM : characterisation testing of hemp shiv to determine the initial water
655 content, water absorption, dry density, particle size distribution and thermal conductivity, Materials
656 and Structures 50. (2017).
657 [56] AFNOR, Hygrothermal performance of building materials and products - Determination of
658 hygroscopic sorption properties, NF EN ISO 12571, (2013), 28 p.
659 [57] C.A. S. Hill, A. Norton, The water vapor sorption behavior of natural fibers, J. App. Polym.
660 Sci. (2009).
661 [58] A. Stamboulis, C. A. Baillie, S. K. Garkhail, H. G. H. Van Melick, T. Peijs, Environmental
662 durability of flax fibres and their composites based on polypropylene matrix, Appl. Compos.
663 Mater. 7 (5–6) (2000) 273–294.
664 [59] EN (European Standards), Tests of fresh concrete. Part 2: Slump test (in Portuguese). EN
665 12350-2, (2009).
666 [60] EN (European Standards), Testing of Fresh Concrete. Part 7: Air Content – Pressure Methods.
667 EN 12350-7 (2009)
668 [61] ASTM C1579-13, Standard Test Method for Evaluating Plastic Shrinkage Cracking of
669 Restrained Fiber Reinforced Concrete (Using a Steel Form Insert), (2013) 1–7.

670 [62] J. Lima, P. Faria, Eco-efficient Earthen Plasters: the Influence of the Addition of Natural
671 Fibers, (eds) Natural Fibres: Advances in Science and Technology Towards Industrial
672 Applications. RILEM Bookseries, Springer, Dordrecht.12 (2016).
673 [63] J. Lima, P. Faria, A, Santos Silva Earth Plasters: The Influence of Clay Mineralogy in the
674 Plasters' Properties, Int. J. Arch. Herit. (2020), https://doi.org/10.1080/15583058.2020.1727064.
675 [64] E. Quagliarini, S. Lenci, The influence of natural stabilizers and natural fibres on the
676 mechanical properties of ancient Roman adobe bricks, J. Cult. Herit. 11 (3) (2010) 309-314,
677 https://doi.org/10.1016/j.culher.2009.11.012 .
678 [65] P. Turcry, A. Loukili, Evaluation of Plastic shrinkage Cracking of self-compacting concrete.
679 Materials Journal, ACI. 103 (4) (2006) 272-280.
680 [66] J. Mora-Ruacho, R. Gettu, A. Aguado, Influence of shrinkage-reducing admixtures on the
681 reduction of plastic shrinkage cracking in concrete, Cem. Concr. Res. 39 (3) (2009) 141-146,
682 https://doi.org/10.1016/j.cemconres.2008.11.011.
683 [67] G. Olivier, R. Combrinck, M. Kayondo, W.P. Boshoff, Combined effect of nanosilica, super
684 absorbent polymers, and synthetic fibres on plastic shrinkage cracking in concrete, Constr. Build.
685 Mater. 192 (2018) 85–98, https://doi.org/10.1016/j.conbuildmat.2018.10.102.
686 [68] I.M.G. Bertelsen, C. Kragh, G. Cardinaud, L.M. Ottosen, G. Fischer, Quantification of plastic
687 shrinkage cracking in mortars using digital image correlation, Cem. Concr. Res. 123 (2019),
688 https://doi.org/10.1016/j.cemconres.2019.05.006 105761.
689 [69] ACI 305R-99, Hot Weather Concreting, ACI Manual of Construction Practice, Part 2,
690 Farmington Hills: American Concrete Institute International, (1999).
691 [70] J.H.J. Kim, C.G. Park, S.W. Lee, S.W. Lee, J.P. Won, Effects of the geometry of recycled
692 PET fiber reinforcement on shrinkage cracking of cement-based composites, Compos. Part B Eng.
693 39 (3) (2008) 442–450, https://doi.org/ 10.1016/j.compositesb.2007.05.001.
694 [71] N. Banthia, R. Gupta, Influence of polypropylene fiber geometry on plastic shrinkage cracking
695 in concrete, Cem. Concr. Res. 36 (7) (2006) 1263–1267,
696 https://doi.org/10.1016/j.cemconres.2006.01.010.

697 [72] R. Paul Borg, O. Baldacchino, L. Ferrara, Early age performance and mechanical
698 characteristics of recycled PET fibre reinforced concrete, Constr. Build. Mater. 108 (2016) 29-47,
699 https://doi.org/10.1016/j.conbuildmat.2016.01.029.